Volcanic evolution of Mount Taylor Stratovolcano, New Mexico: Facts and misconceptions

Fraser Goff, William McIntosh, Lisa Peters, John A. Wolff, Shari A. Kelley, Cathy J. Goff, and G. Robert Osburn

2021, pp. 117-128. https://doi.org/10.56577/FFC-71.117

in:

Geology of the Mount Taylor area, Frey, Bonnie A.; Kelley, Shari A.; Zeigler, Kate E.; McLemore, Virginia T.; Goff, Fraser; Ulmer-Scholle, Dana S., New Mexico Geological Society 71st Annual Fall Field Conference Guidebook, 310 p. https://doi.org/10.56577/FFC-71

This page is intentionally left blank to maintain order of facing pages.

New Mexico Geological Society Guidebook, 71st Field Conference, Geology of the Mount Taylor Area, 2021, p. 117-128.

VOLCANIC EVOLUTION OF MOUNT TAYLOR STRATOVOLCANO, NEW MEXICO: FACTS AND MISCONCEPTIONS

Fraser Goff[1], William McIntosh[1,2], Lisa Peters[2], John A. Wolff[3], Shari A. Kelley[2], Cathy J. Goff[4], and G. Robert Osburn[5]

[1]Department of Earth and Environmental Science, New Mexico Tech, 801 Leroy Place, Socorro, NM 87801; candf@swcp.com
[2]New Mexico Bureau of Geology and Mineral Resources, 801 Leroy Place, Socorro, NM 87801
[3]School of the Environment, Washington State University, Pullman, WA 99164
[4]Independent Consultant, 5515 Quemazon, Los Alamos, NM 87544
[5]Earth and Planetary Science, Washington University, St. Louis, MO 63130

Abstract—Mount Taylor (3445 m elevation) developed from roughly 3.2 to 2.5 Ma and is a composite stratovolcano (Mount Taylor stratovolcano, MTS) composed of coalesced basaltic trachyandesite to rhyolite domes, flows, plugs, dikes, interlayered ash, and comingled debris flows. The main edifice is surrounded by later cones and flows of (mostly) trachybasalt that erupted until 1.27 Ma. Contrary to previous interpretations, the summit trachyandesite flows of MTS (2.75 to 2.72 Ma) are not the youngest eruptions on the edifice. A variety of satellite domes, flows, radial dikes and a central plug of mostly trachydacite were intruded and erupted until 2.52 Ma. Thus, also contrary to previous studies, the youngest eruptions at MTS are not "andesitic." An elongate, eastward-facing Amphitheater about 6.5 km long formed in the approximate center of MTS late in its development. The best explanation for formation of the MTS Amphitheater is erosion by mass wasting and fluvial incision. This feature did not form from large, centralized, late stage explosions, from Mount St. Helens-type lateral blasts with associated fall and ignimbrite, or from Pleistocene glaciation of the edifice, although it may have formed in part from an unrecognizable debris avalanche. Previous studies have speculated that MTS developed a single cone or bulbous dome that once attained a height of 4270 m, but it is more probable that the mixture of small, coalesced vents and domes forming the original summit never rose above 3800 m. Using this maximum elevation, an average diameter of 16 km for the volcano from recent mapping, and the formula for a right circular cone, the estimated volume of MTS is 85 $km^3 \pm 20\%$. From this volume and the time span of intense MTS construction (0.76 Ma), the average eruptive (magmatic) flux rate is about 0.11 km^3 per 10^3 years. These values for MTS are small compared to those of Cascades-type subduction zone stratovolcanoes, such as Mount St. Helens.

INTRODUCTION

Mount Taylor is an extinct composite stratovolcano that is part of the greater Mount Taylor–Mesa Chivato volcanic field (Hunt, 1938; Crumpler, 1980a, b) and is one of many volcanic fields that define the northeast-trending Jemez Lineament (JL, Figs. 1, 2; Mayo, 1958; Luedke and Smith, 1978; Goff and Kelley, 2020). Mount Taylor stratovolcano (MTS, 3445 m) forms a conspicuous topographic feature roughly 20 km northeast of Grants and is New Mexico's second largest late Cenozoic volcanic complex after the Valles caldera and Jemez Mountains (Crumpler, 2010). The peak is sacred to the nearby Acoma, Laguna and Zuni pueblos and is known as "Turquoise Mountain," or *Tso Tzil*, to the Diné (Navajo). The present name honors President Zachary Taylor, a major general who became U.S. president in March 1849 and who died prematurely in office in July 1850.

Many researchers have mapped and conducted volcanic and petrologic studies at Mount Taylor starting with Dutton (1885); see Goff et al. (2019) for a comprehensive list. Because of the abundant uranium resources hosted in Jurassic rocks beneath and around the volcano, the New Mexico Bureau of Geology and Mineral Resources produced a series of 7.5-minute geologic quadrangles beginning in 2007 (Goff et al., 2008, 2012, 2014a; McCraw et al., 2009; Osburn et al., 2010; Skotnicki et al., 2012), which resulted in a detailed 1:36,000-scale compilation of the Mount Taylor and southwest Mesa Chivato region (Goff et al., 2019). During this mapping, 107 new $^{40}Ar/^{39}Ar$ dates and 216 new major and trace element chemical analyses were obtained. Toward the end of the mapping campaign, we also employed a portable flux gate magnetometer to acquire magnetic polarities of important volcanic units. The polari-

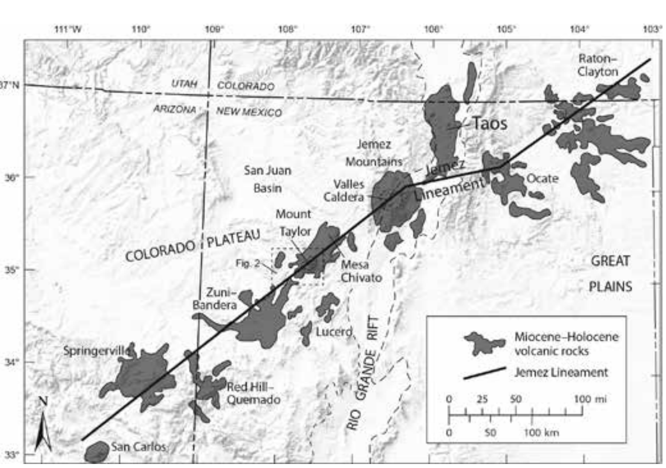

FIGURE 1. Map showing the location of Mount Taylor with respect to other volcanic fields of the Jemez Lineament, to the San Juan Basin, and to basins of the Rio Grande rift. Inset shows location of Figure 2. Modified from Goff et al. (2019).

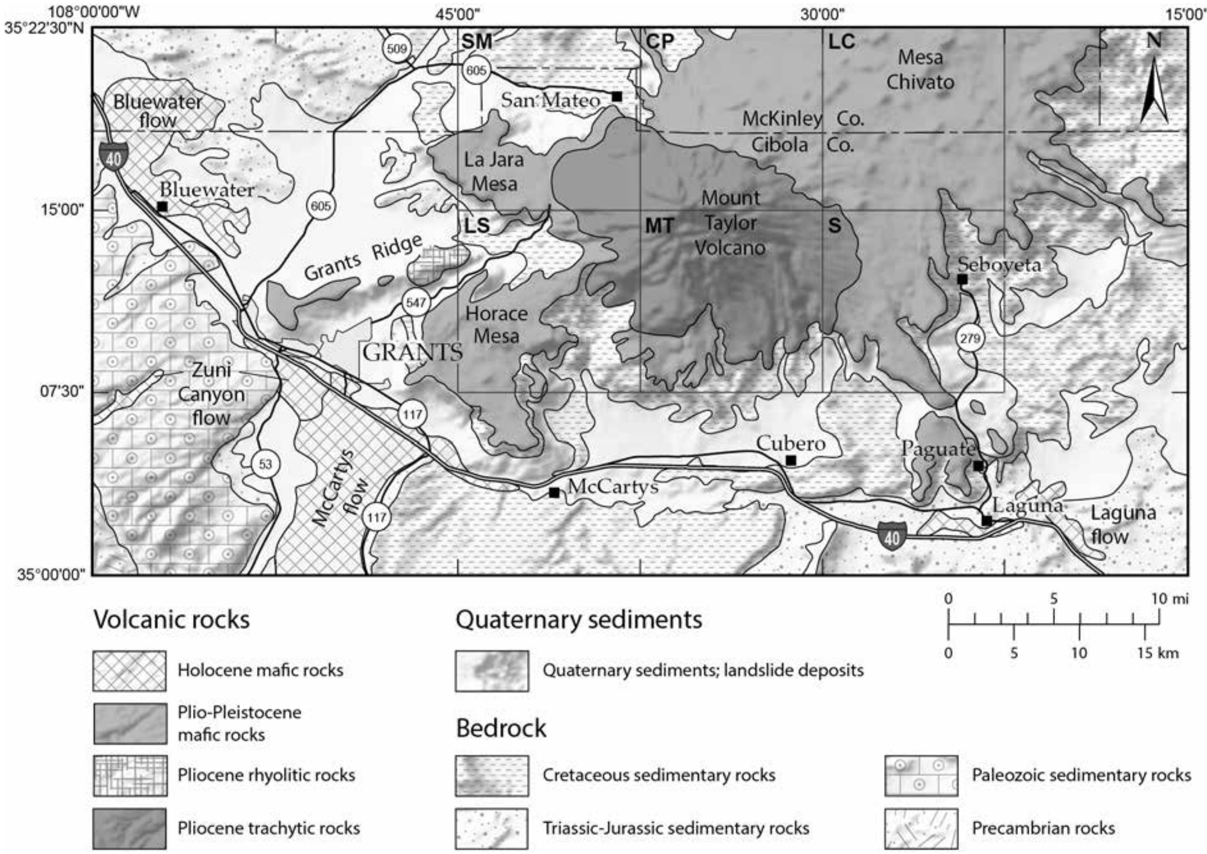

FIGURE 2. Map of Mount Taylor volcano region showing simplified geology and locations of six recently completed 1:24,000 quadrangles: CP = Cerro Pelón, LC= Laguna Cañoneros, LS = Lobo Springs, MT = Mount Taylor, S = Seboyeta, and SM = San Mateo. Modified from Goff et al. (2019).

ties provided an independent check on the dates (see booklet in Goff et al., 2019, for all radiometric and magnetic polarity results). This paper summarizes the geology, dates, chemistry and magnetic polarities of MTS, presents a revised volcanic evolution for its development, and comments on the origin of MTS Amphitheater (Fig. 3). Volcanism on Mesa Chivato and Grants Ridge is not covered herein.

GEOLOGIC BACKGROUND

Jurassic and Cretaceous non-marine and marine sedimentary rocks underlie MTS and Cretaceous strata interfinger with each other around and beneath MTS. The Jurassic Westwater Canyon Member of the Morrison Formation is host to abundant uranium ores that made the Grants district the largest uranium-producing area in the United States from 1951–1980. This district still ranks second in the United States in uranium reserves (Kelley, 1963; McLemore, 2011; McLemore and Chenoweth, 2017). Several hundred boreholes drilled by mining companies through volcanic rocks west and north of MTS traced uranium-bearing Jurassic strata beneath the volcano flanks east of the Mt. Taylor Mine at San Mateo (Goff et al., 2019). The upper Cretaceous section is a transgressive–regressive sequence (Sears et al., 1941; Kelley, 1963; Owen and Owen, 2003) that records a gradual transition from open marine conditions to marginal marine and deltaic settings. Coal production from Upper Cretaceous strata in the map area covered by Goff et al. (2019) was small and limited to the eroded basins south and southwest of MTS (Hoffman, 2017, fig. 10).

MTS overlies the southeast margin of the Laramide San Juan Basin and also lies in a transition zone of extension between the Colorado Plateau to the northwest and the Rio Grande rift (RGR) to the east (Olsen et al., 1979; 1987; Thompson and

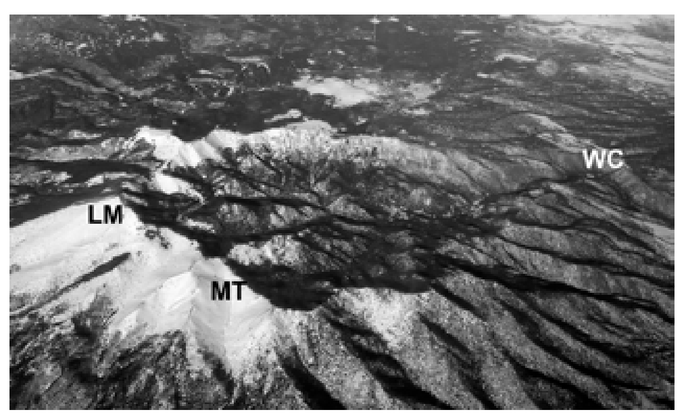

FIGURE 3. Photo taken from an airplane during the winter of 2008 looking northeast across the Amphitheater of MTS toward Mesa Chivato; LM = La Mosca, MT = Mount Taylor; WC = Water Canyon. Photo courtesy of Kirt Kempter.

Zoback, 1979; Aldrich and Laughlin, 1984). Recent interpretation of 3D seismic structure beneath the RGR to a depth of 200 km (Sosa et al., 2014) suggests that the transition zone is a broad low velocity region and that an upwelling sheet or linear bulge of hot mantle material underlies the JL. This upwelling mantle sheet has probably fed the volcanic centers along the JL, including Mount Taylor and Mesa Chivato (Fig. 1).

ANALYTICAL METHODS

Recent mapping of Mount Taylor and surrounding areas was enhanced by petrographic examination of 150 polished thin sections. These observations constrain mineral assemblages and textures in many volcanic units and allow us to assign rock names to units that were not chemically analyzed. Phenocrysts in MTS eruptive products are similar to those in mildly alkalic volcanic terrains erupted in or near some continental rifts (Table 1; Wilson, 1989, fig. 11.12).

In this paper, we highlight 62 of 107 $^{40}Ar/^{39}Ar$ dates (Table 2) obtained during the 2007–2013 quadrangle mapping projects, including only those dates that illustrate the development and evolution of MTS proper. Dates from the Grants Ridge rhyolite center and greater Mesa Chivato are not discussed herein (see Goff et al., 2019, for these results). All dates in Table 2 are calculated using the Fish Canyon Tuff sanidine neutron flux interlaboratory monitor (FC-2) with an assigned age of 28.201 Ma (Kuiper et al., 2008).

To help constrain our geochronology, we measured the magnetic polarity of many samples by handheld (portable) fluxgate magnetometer (all rock types) and Brunton™ compass (basaltic rocks only; Table 2). We used a µMAG™ digital magnetometer built by MEDA, Inc. (Dulles, VA). Many volcanic rocks in the Mount Taylor region were erupted during the magnetic polarity flip from the Gauss Normal Chron to the Matuyama Reverse Chron at 2.581 Ma (Gee and Kent, 2007, table 3). Unfortunately, our magnetic polarity measurements started late in the mapping campaign and many hard-to-access locations were not revisited. Note that this report employs the Plio–Pleistocene boundary of 2.58 Ma in accordance with recent international stratigraphic changes (Cohen et al., 2013).

We also acquired 216 major and trace element chemical analyses of volcanic rocks in the Mount Taylor region using a combination of XRF and ICP-MS methods and analyzed by Washington State University (Fellah, 2011) and ALS Laboratories (Reno, Nevada, see their website for methods). Table 2 lists normalized silica and total alkali contents of 56 dated map units that were key in constraining the evolution of MTS. Complete geochemical data and interpretations will be published at a future time.

VOLCANIC EVOLUTION, MOUNT TAYLOR STRATOVOLCANO

Previous Work

Previous investigations of MTS rocks were conducted by Hunt (1938), Baker and Ridley (1970), Lipman and Moench (1972), Lipman and Mehnert (1979), Crumpler (1982), and Perry et al. (1990). The alkalic (i.e., $Na_2O + K_2O$–rich) chemistry of MTS rocks was noted by all researchers except Baker and Ridley (1970), who mistakenly called the rocks "calc-alkaline." Through the years, rock classification schemes (i.e., "rock names") used by past workers have varied widely, leading to considerable confusion (see Goff et al., 2019, p. 6). Beginning with Hunt (1938), all subsequent studies claimed that the youngest eruptions of the MTS are those that form the high-elevation stack of lavas at the summit (i.e., Mount Taylor proper). Consequently, all previous researchers (e.g., Crumpler, 2010, p. 57) have stated that the youngest MTS summit flows are "andesitic to latitic" in mineralogy and chemistry, post-dating all earlier eruptions of "dacite, quartz latite and rhyolite." As noted below, our investigation revealed a different sequence of eruptions.

Rock Classification from Chemistry

For our Mount Taylor project (Table 1 and Fig. 4), we have used the internationally accepted classification scheme of Le Bas et al. (1986), previously published chemistry, and our own chemical analyses to rename and categorize the volcanic units.

TABLE 1. Phenocryst mineralogy of volcanic rocks, Mount Taylor stratovolcano, New Mexico (Goff et al., 2019).

	Basanite	Basalt	Tbasalt	Tandesite	Trachyte	Tdacite	Rhyolite
Olivine	X	X	X	x		tr	
Analcime	x						
Augite	X	X	X	X	x	X	x
Hypersthene			x	x		x	
Hornblende			x	X	X	X	x
Biotite			tr	x	X	X	X
Plagioclase	X	X	X	X	X	X	x
K-Feldspar				x	x	X	X
Quartz				tr		x	X

X = major, x = minor, tr = trace; Tbasalt = trachybasalt, Tandesite = trachyandesite, Tdacite = trachydacite.

TABLE 2. Summary of $^{40}Ar/^{39}Ar$ dates, magnetic polarities, silica and total alkalis for Mount Taylor stratovolcano.

Site See Fig. 6	Map Unit [1]	Rock Type [2]	Location UTM NAD 27	Ar^{40}/Ar^{39} Lab No.	Phase[3]	Age Analysis[4]	Steps/ Analyses	Age (Ma)[5] ± 2σ	MSWD[6]	Magnetic Polarity[7]	Age Match[8]	Silica[9] (norm)	TAS[9] (norm)
Phase 4: Terminal mafic volcanism													
1	Qyatb	Aphyric tbasalt, Cerro Pelon	026668 390562	59077	Gdm	LTF	6	1.27±0.19	10.78	nd		49.18	6.84
2	Qfqtb	Qtz-bearing tbasalt	0269195 3905411	59754	Gdm	LSH	8	1.54±0.07	1.60	nd		49.51	5.10
3	Qfqtb	Qtz-bearing tbasalt	0258356 3900247	62196	Gdm	LSH	7	1.65±0.04	2.70	R (brun)	yes	48.78	5.20
4	Qyh	Aphyric tbasalt	0264574 3907479	63320	Gdm	BSH	7	1.73±0.02	3.45	confused	lightning	na	na
5	Qyxtb	Xenocrystic tbasalt	025843 390625	58995	Gdm	LSH	9	1.75±0.03	1.80	R (fgate)	yes	48.73	5.82
6	Qatc/Qatb	Aphyric tbasalt	0266761 3908202	59755	Gdm	LSH	8	1.77±0.05	1.18	nd		na	na
7	Qyxtb	Xenocrystic tbasalt	0260840 3917200	58996	Gdm	LSH	8	1.80±0.05	2.80	N (brun)	yes	48.85	5.98
8	Qatd/Qatb	Horace Mesa dike and flow	0257002 3896823	63322	Gdm	BSH	5	1.80±0.01	5.57	N (fgate)	yes	48.38	6.09
9	Qyxtb	Xenocrystic tbasalt	0269287 3904689	59211	Gdm	LSH	10	1.86±0.06	1.93	R(brun)	yes	48.99	5.63
off map N	Qyptb	Gabbro-bearing tbasalt	0267619 3913003	59080	Gdm	LTF	7	2.31±0.13	8.83	R (fgate)	yes	49.09	5.69
10	Qyfpb	Fine-grained tbasalt	0268705 3907280	59213	Gdm	LSH	9	2.38±0.14	3.70	nd		47.60	5.06
Phase 3: Youngest Summit, Amphitheater and Satellite Euptions													
11	Qxgi	Oliv gabbro plug	0267302 3901456	62193	Gdm	LSH	8	1.98±0.05	1.57	nd		47.82	4.90
12	Teta	Enclave tandesite	0261548 3899333	58056	San	LSH	4	2.52±0.07	4.85	R (fgate)	yes	61.38	7.72
13	Tsptd	"Spud Patch" tdacite	0265508 3907887	59081	Gdm	LTF	5	2.55±0.06	3.76	R (fgate)	yes	62.28	9.17
14	Tqtd	Intrusion interior	0264093 3902080	58728	San	LTF	14	2.56±0.02	1.31	R (fgate)	yes	68.61	8.88
15	Tqtd	Intrusion west margin	0263623 3901970	58727	San	LTF	8	2.60±0.02	1.83	R (fgate)	yes	71.11	9.52
Phase 3: Amphitheater Dikes													
16	Thbi	Tdacite, east Amph	0267629 3900865	59112	Bio	LSH	6	2.66±0.06	2.60	N(fgate)	yes	62.78	9.85
17	Tbi	Tdacite west Amph	0263507 3903038	63722	San	LSH	13	2.66±0.01	1.47	nd		67.98	10.83
18	Thbi	Tdacite west Amph	0263207 3903088	63688	Bio	BSH	16	2.67±0.01	1.07	nd		63.31	9.81
19	Tbhd	Tdacite NW Amph	0264782 3903958	63687	Bio	BSH	16	2.67±0.01	2.07	nd		63.42	9.29
20	Tbi	South Wall Tdacite dike	026632 390015	59003	Bio	LSH	11	2.71±0.03	1.40	nd		64.69	10.27
21	Tbi	Tdacite SE Amph	0265107 3900783	59004	Bio	LSH	9	2.79±0.02	0.60	nd		66.68	10.61
22	Tbi	Tdacite, intrudes rhyolite	0265667 3901451	59072	Plag/San	LSH	13	2.80±0.06	2.60	nd		na	na
Phase 3: Satellite Domes and Plugs													
23	Thta	Hbd tandesite W flank	0257095 3903685	58069	Plag	LSH	10	2.62±0.10	0.90	N (fgate)	yes	60.83	9.04
24	Tbd	Tdacite N Amph rim	0266058 3903990	63360	Gdm	BSH	6	2.66±0.01	5.75	N (fgate)	yes	63.77	9.44
25	Thtd	Hbd tdacite NW flank	0262388 3904802	63364	Hbd	BSH	4	2.66±0.02	1.83	N (fgate)	yes	62.37	9.57
26	Tbhtd	Porphyritic tdacite NW flank	0261430 3905862	63362	Bio	BSH	3	2.66±0.01	1.84	N (fgate)	yes	62.72	9.38
27	Tpota [10]	Oliv tandesite NE Amph rim	0268534 3903124	58999	K-feld	LSH	13	2.69±0.04	1.20	nd		62.04	9.11
off map E	Tpota [10]	Oliv tandesite, flow end	0272753 3901225	61215	Gdm	LSH	8	2.69±0.01	1.97	nd		na	na
28	Tbhtd	Tdacite plug S flank	0260199 3898207	59765	Bio	LSH	9	2.70±0.03	2.27	N (fgate)	yes	64.37	9.50
29	Ttdc	Porphyritic tdacite SE rim	0268263 3900104	59001	K-feld	LSH	9	2.72±0.04	1.90	nd		na	na
Phase 3: Mount Taylor and La Mosca													
30	Thta	Tandesite below MT summit	0262890 3902543	62195	Gdm	LSH	11	2.72±0.02	1.65	N (fgate)	yes	57.91	8.37
31	Tsetd	Porphyritic tdacite NW flank	0262306 3907190	59083	Plag	LSH	6	2.73±0.06	1.61	N (fgate)	yes	62.52	9.43
32	Tpbti/Tpbtd	Tdacite intrusion La Mosca	026369 390413	59089	K-feld	LSH	8	2.73±0.03	1.98	nd		66.28	10.64
33	Thtas	Tandesite MT summit	0262711 3902326	62191	Gdm	LSH	7	2.75±0.01	int age	confused	lightning	59.69	8.85

TABLE 2. Continued.

Site See Fig. 6	Map Unit [1]	Rock Type [2]	Location UTM NAD 27	Ar^{40}/Ar^{39} Lab No.	Phase[3]	Age Analysis[4]	Steps/ Analyses	Age (Ma)[5] $\pm 2\sigma$	MSWD[6]	Magnetic Polarity[7]	Age Match[8]	Silica[9] (norm)	TAS[9] (norm)
Phase 2: Older lavas and domes													
34	Tpb	Classic plag basalt	0262853 3896155	58741	Gdm	FSH	5	2.78±0.06	2.80	confused		50.64	5.89
35	Tptd	Porphyritic plag tdacite	0263193 3898119	58736	Bio	FSH	11	2.80±0.05	2.03	N (fgate)	yes	62.28	9.24
36	Tpb	Classic plag basalt	026734 390269	58997	Gdm	LSH	5	2.81±0.04	2.30	N (fgate)	yes	51.25	6.13
37	Ttai	Oliv tandesite dike	026011 390771	58998	Gdm	LSH	7	2.81±0.03	1.00	nd		57.57	8.57
38	Ttd	Tdacite Rinconada Can	0259159 3898891	59768	Plag	LSH	11	2.81±0.14	1.59	nd		64.12	9.76
39	Tpetd	Enclave tdacite W flank	0260635 3904813	59002	K-feld		8	2.83±0.04	Isochron	N (fgate)	yes	63.57	9.74
40	Tcpt	Porphyritic trachyte W flank	0260825 3903942	59733	San	LSH	15	2.84±0.08	1.12	nd		67.68	11.54
41	Tbht	Bio-hbd trachyte S flank	0264679 3898779	59217	Plag	LSH	9	2.85±0.04	1.36	nd		65.94	10.92
42	Tplta	Plag tandesite NW flank	026143 391001	58994	Gdm	LSH	7	2.88±0.04	1.30	nd		62.22	9.15
Phase 1 (late) to Phase 3 (early): Pyroclastic rocks													
off map E	Ttdt	Pumice, fall deposit	0277885 3897421	61250	San	LSH	11	2.717±0.002	2.42	nd		69.33	9.85
43	Ttdt	Pumice tdacite ignimbrite	0258260 3901541	58057	Bio	LSH	4	2.73±0.06	1.90	nd		64.79	9.10
44	Twst	Pumice ignimbrite SE flank	0268252 3898323	59069	San	LSH	15	2.76±0.03	2.00	nd		na	na
45	Twst	Pumice in undivided tuffs	0270509 3895944	59068	San	LSH	15	2.78±0.03	1.00	nd		69.59	9.90
46	Ttdt	Pumice tdacite ignimbrite	026219 390893	59006	Plag	LSH	7	2.81±0.09	1.70	nd		62.77	8.71
47	Twst	Pumice in undivided tuffs	0270509 3895944	59067	San	LSH	9	2.85±0.07	3.30	nd		na	na
48	Twst	Pumice in undivided tuffs	0270891 3896290	59071	San	LSH	14	2.89±0.04	2.00	nd		66.55	8.98
off map N	Twst	Pumice, fall despost	026846 391648	59218	Plag	LTF	20	3.06±0.12	2.41	nd		65.35	7.99
49	Trt	Pumice, fall desposit	0259632 3911188	59005	Bio	LSH	5	3.10±0.20	5.90	nd		74.07	9.41
Phase 1: Mount Taylor floor													
50	Tre	East Amph rhyolite	0265885 3902701	59070	San	LSH	12	2.93±0.04	0.80	nd		68.67	11.56
51	Trw	West Amph rhyolite	0263405 3902479			K/Ar date, Perry et al, 1990		3.03±0.11				73.79	8.60
52	Ttr	Trachyte, east Amph	0267973 3901341	62185	Gdm	LSH	7	3.16±0.01	0.9?	nd		61.02	10.85
53 [11]	Toab	Alkali basalt Water Can	0273250 3894422	61226	Gdm	LSH	10	3.18±0.04	3.27	N (fgate)	yes	48.01	4.62
off map N	Totb	Aphyric tbasalt	0263545 3914403	59212	Gdm	LSH	7	3.22±0.06	0.52	R (brun)	yes	47.85	5.41
54	Toab	Alkali basalt plug S flank	0260052 3898385	59756	Gdm	LSH	9	3.23±0.12	1.76	R (fgate)	yes	46.39	4.56
55	Tbaa	Amph basanite	0266680 3902034	62189	Gdm	LSH	4	3.24±0.04	1.32	nd		43.60	5.35
56	Tbhtd	Tdacite, Riconada Canyon	0260986 3898996	58070	WR	LSH	5	3.28±0.20	8.50	N (fgate)	yes	63.88	9.82
57	Tbaw	West basanite, Lobo Can	025805 390129	58073	WR	LSH	6	3.66±0.15	2.60	R (fgate)	yes	44.37	6.95
off map SE	Tbae	East basanite SE flank	0277203 3894190	61227	Gdm	LSH	10	3.74±0.02	1.55	R (fgate)	yes	44.33	5.58

[1]From geologic map of Goff et al. (2019)
[2]Tbasalt = trachybasalt, Tandesite = trachyandesite, Tdacite = trachydacite
[3]Bio = biotite, Gdm = groundmass, Hbd = hornblende, K-Feld = K-feldspar, Plag = plagioclase, San = sanidine, WR = whole rock
[4]LTF = laser total fusion, LSH = laser step heat, FSH = furnace step heat, BSH = bulk step heat
[5]Mean Square Weighted Deviation
[6]All dates use the Fish Canyon Tuff sanidine neutron flux interlaboratory monitor (FC-2) with an assigned age of 28.201 Ma (Kuiper et al., 2008).
[7]N = normal polarity, R = reverse polarity, brun = brunton compass, fgate = flux gate magnetometer, nd = not determined
[8]Polarity and age match within error of the date (see Gee and Kent, 2007, or Goff et al., 2019, table 2).
[9]Silica = SiO_2, normalized wt%, TAS = total alkalis, $Na_2O + K_2O$, normalized wt%, na = not analyzed
[10]Unit Tpota was dated at two different locations several kilometers apart to verify age continuity.
[11]Date site is off map to southeast but unit is exposed in Water Canyon.

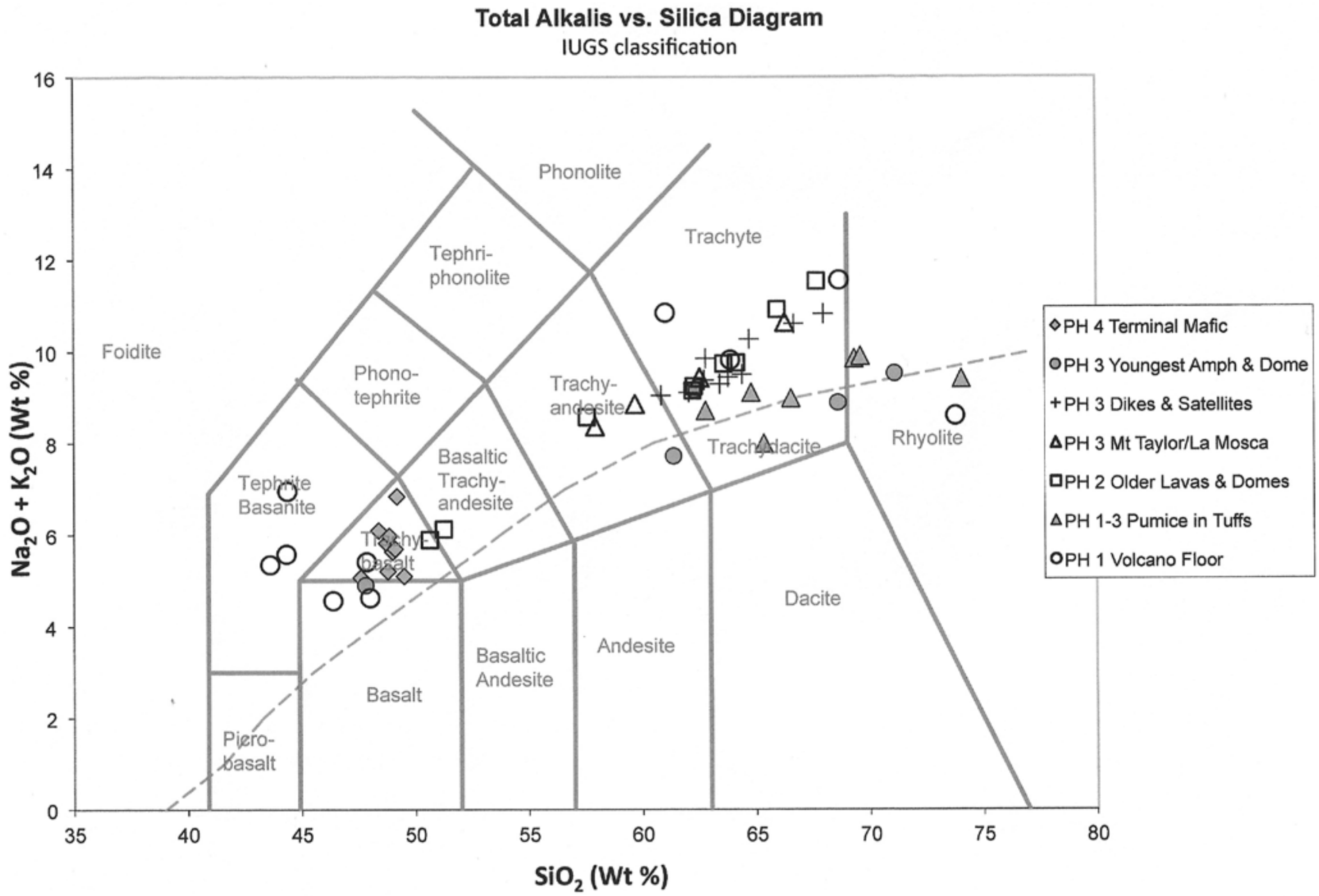

FIGURE 4. Total alkali versus silica plot for MTS rocks listed in Table 2 (Le Bas et al., 1986). Dashed line separates alkaline (top) from calc-alkaline rocks (Irvine and Baragar, 1971). Age ranges: Phase 1, 3.74–2.90 Ma; Phase 2, 2.90–2.75 Ma; Phase 3, 2.75–2.53 Ma; Phase 4, 2.50–1.27 Ma. Amph = Amphitheater.

Thus, most alkali basalts (hawaiites) are now called trachybasalts; basaltic andesites (mugearites) are called basaltic trachyandesites; andesites (latites) are called trachyandesites; and quartz latites are called trachydacites. The only volcanic rocks that we have not renamed are rhyolites and basanites, although we reserve the name trachyte for a few of the most alkali-rich rocks that plot in the trachydacite-trachyte field (Fig. 4).

The total-alkali versus silica plot (Fig. 4) displays the restricted group of dated MTS samples prepared for this paper (Table 2; see Fellah, 2011, fig. 8 or Goff et al., 2019, fig. 8 for comprehensive plots that include Grants Ridge and Mesa Chivato). Figure 4 shows a fairly linear trend between basalt/trachybasalt and trachydacitic end-members. Basanites form a separate group, and there is a separate trend for pyroclastic rocks and rhyolites, with the caveat that such rocks may have lost alkali elements during post-eruptive weathering or alteration. Note that, for the most part, MTS rocks are alkalic, not calc-alkalic as previously stated by Baker and Ridley (1970).

Construction of Mount Taylor Stratovolcano

Our new dates and magnetic polarity measurements indicate that the main edifice and satellite domes of MTS were erupted from about 3.2–2.5 Ma, more or less in agreement with previous researchers, although dissimilar in many details (Lipman and Mehnert, 1979; Perry et al., 1990; Crumpler, 2010). Thus, construction of MTS was essentially complete by the end of the Pliocene at 2.5 Ma, but erosion since that time has decapitated the highest points of the original complex and carved out the Amphitheater (Fig. 3).

MTS is surrounded by and interlayered with mostly mafic lava flows, scoria cones, and a few centers of more silicic composition, which are not discussed further in this paper. Overall, the most common mafic rock is trachybasalt (hawaiite). The few eruptions of basanite and basalt generally occur relatively early in the eruptive history, while trachybasalt is predominant in later eruptions (Figs. 4, 5, 6).

Our dates and those of others show that initial but sporadic volcanism in the Mount Taylor region began at about 4.49±0.08 Ma (Picacho Peak basanite plug and dikes; Hallett et al., 1997) and ended at about 1.27±0.19 Ma (Cerro Pelón trachybasalt cone and flow). Again, this age range generally agrees with the range determined by previous researchers (e.g., Lipman and Mehnert, 1979), but the details are considerably different.

What follows are descriptions of the four phases of eruptions that formed the MTS. Unit name identifiers are from Goff et al. (2019).

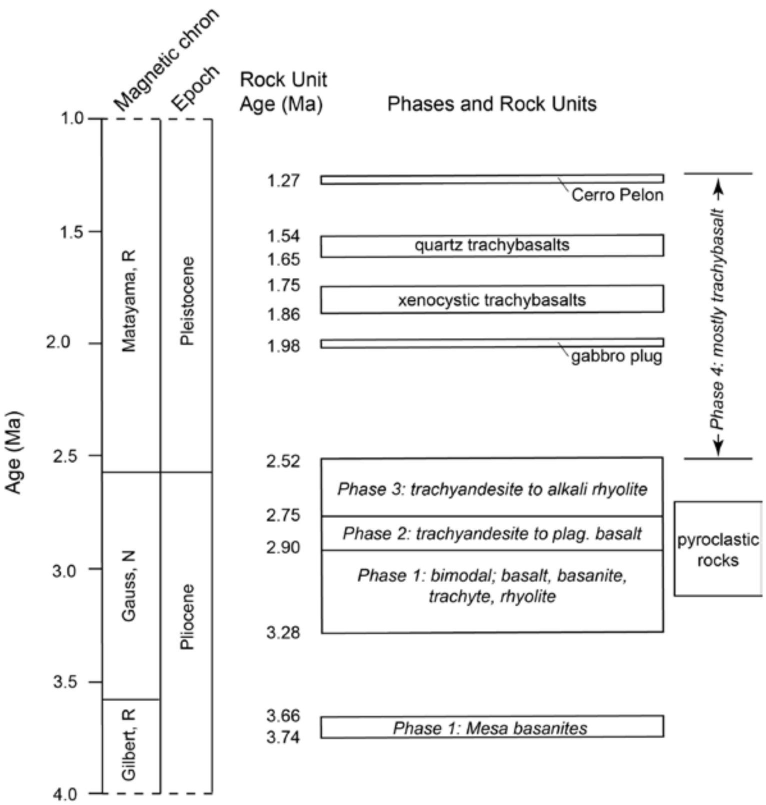

FIGURE 5. Diagram showing the evolution of MTS compared to major magnetic polarity intervals (Chron: see text); ages and rock names from Table 2; plag. = plagioclase.

Phase 1, the volcano floor (3.74–2.93 Ma)

Phase 1 volcanism (Figs. 5, 6) began with the eruption of two widespread flows of basanite that initially formed mesa caps (units Tbae and Tbaw, 3.74–3.66 Ma, Table 2), as documented by previous workers (Lipman and Moench, 1972; Perry et al., 1990). Next came eruption of a trachydacite dome exposed in the bottom of upper Rinconada Canyon (unit Tbhtd). The date for this unit (3.28±0.20 Ma) has a relatively large error, but the magnetic polarity is normal, suggesting an age <3.22 Ma (Table 2). Following emplacement of this dome, another widespread eruption of basanite occurred in the eastern sector of the present Amphitheater (unit Tbaa, 3.24±0.04 Ma), as well as eruptions of alkali basalt (unit Toab, 3.23±0.12 and 3.18±0.04 Ma), now exposed in upper Rinconada Canyon and in the bottom of the central to eastern Amphitheater. Both the later basanite and coeval flows of alkali basalt flowed many kilometers down ravines associated with an earlier Water Canyon (not shown on Fig. 6 for clarity; see Goff et al., 2019). Within what is now the eastern Amphitheater, a small trachyte dome (unit Ttr, 3.16±0.01 Ma) was erupted, followed by emplacement of rhyolite domes and intrusions in the western and central Amphitheater (units Trw and Tre, 3.03±0.11 and 2.93±0.04 Ma, respectively). Small volume rhyolite to trachydacite ignimbrite and fall deposits (units Trt, 3.10±0.20 Ma, and Twst, ranging from 3.04–2.74 Ma) filled early paleocanyons and paleoravines, particularly in the Water and San Mateo canyon areas, and sporadically covered mesa tops around the volcano (Dunbar et al., 2013; Kelley et al., 2013). Products of individual pyroclastic eruptions are <1 km^3 in volume and probably originated during silicic dome eruptions. No large pyroclastic deposits, vents, craters or caldera have been identified at MTS, although thickness trends point to a source or sources in the west-central part of the early edifice.

Phase 2, the stratovolcano grows (2.88–2.78 Ma)

During phase 2, the growing stratovolcano erupted a mixture of trachyandesite, trachydacite, and trachyte lavas and domes, and associated small volume ignimbrites and tuffs (Figs. 4, 5, 6). Two previously unrecognized trachytes (Tbht and Tcpt; Table 2) were dated at 2.85±0.04 and 2.84±0.08 Ma, respectively. The second trachyte is overlain by a thick trachydacite flow (unit Tpetd) dated at 2.83±0.04 Ma, which contains abundant mafic enclaves. Field relations and other dates bracket the early Phase 2 dome eruptions to be between 2.88 and 2.78 Ma. Small volume ignimbrites (e.g., unit Ttdt ranging from 2.81 to 2.73 Ma) continued to fill in preexisting ravines and depressions and are also found in scattered outcrops around the volcano interlayered with trachybasalt and minor basalt lavas, and with early volcaniclastic rocks shed off the developing volcano.

The defining units ending Phase 2 consist of a series of "plagioclase" or "big feldspar" mafic eruptions, often called "plagioclase basalt" (2.81–2.78 Ma). Baker and Ridley (1970) first described these flows. What we call classic plagioclase basalts (Table 2, Figs. 4, 5, 6) are borderline trachybasalt to basaltic trachyandesite in composition. We found that most MTS rocks previously called plagioclase basalt range from basaltic trachyandesite to trachyandesite in composition (Goff et al., 2019). The classic varieties are among the latest eruptions of this group, but these rocks are interlayered within the uppermost intermediate flows making up Phase 2 (e.g., unit Tptd dated at 2.80±0.05 Ma). "Plagioclase basalt" is most common on the central to eastern flanks of MTS, exposed in canyons cutting its southern flank, and on the bluff east of San Mateo Basin.

Phase 3, the final stratovolcano eruptions (2.75–2.52 Ma)

Continued effusion of intermediate composition lavas and domes from 2.75–2.52 Ma characterized volcanic activity for Phase 3. These eruptions originated in part from a composite stock generating radial dikes that developed beneath the central to western Amphitheater (Fig. 6). Our new dates and chemical analyses show that trachyandesite and trachydacite were coeval in time and space. For example, what is now the Mount Taylor summit was built of successive flows of hornblende trachyandesite (units Thta and Thtas, 2.75±0.01 to 2.72±0.02 Ma) erupted from a buried or obliterated vent in the western Amphitheater. "La Mosca" (3,365 m; Fig. 3) is constructed by a small intrusion exposed in the northwest Amphitheater wall (unit Tpbti, 2.73±0.03 Ma) that produced a thick flow of trachydacite (Tpbtd). These are presently the two highest peaks of MTS, but

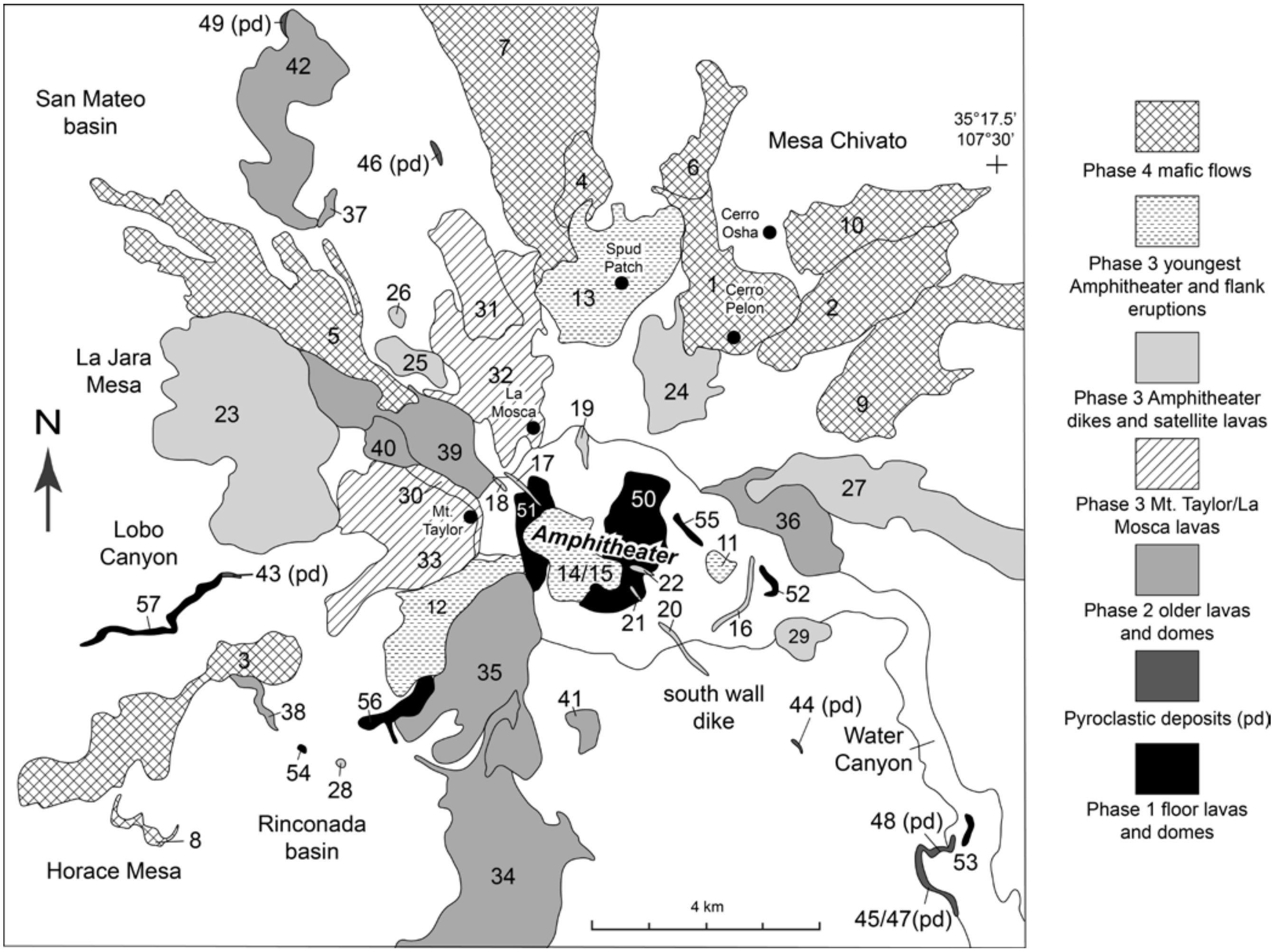

FIGURE 6. Sketch map showing location of MTS rocks according to evolutionary phase of the volcano (Fig. 5). Numbers correspond with location numbers of samples in Table 2, column 1.

due to subsequent erosion, the maximum height of the edifice was higher than now.

During this period, eruptions of ignimbrite and pyroclastic fall deposits virtually ceased. A trachydacite ignimbrite at the head of Lobo Canyon (unit Ttdt) previously identified by Lipman and Mehnert (1979) was dated at 2.73±0.06 Ma. The youngest pyroclastic deposit we found was a relatively thin trachydacite to alkali rhyolite fall deposit east of MTS (e.g., unit Ttdt, 2.717±0.002 Ma). A few dome collapse breccias (glowing avalanche deposits?) are recorded in the larger dome eruptions (i.e., sugary enclave trachydacite, unit Tsetd), but such deposits appear to be a minor component of MTS. In contrast, rapid erosion of the growing volcano formed large aprons and fans of water-transported debris flows and other volcanic sediments interlayered with lava flows. These deposits radiate in all directions away from the volcano, but are thickest to the east and southeast toward the ancestral drainage of the Amphitheater. Possibly, the debris flow sequence contains unrecognizable debris avalanche deposits from Phase 3 domes.

Toward the middle to end of Phase 3 (2.72–2.52 Ma), a series of satellite domes and flows erupted on the margins and flanks of the volcano (e.g., unit Tpota, 2.69±0.02 Ma, average of two dates). These eruptions are mostly trachydacite (Table 2) and match the chemistry and age of several radial dikes exposed within and on the margins of the Amphitheater (2.71 to 2.66 Ma). The last magmatic products emitted from the composite stock are: 1) a trachydacite to alkali rhyolite plug intruded into the western Amphitheater (unit Tqtd, 2.60±0.02 to 2.56±0.02 Ma); 2) the Spud Patch trachydacite satellite dome, erupted on the northern flank of MTS (unit Tsptd, 2.55±0.06 Ma); and 3) an enclave-rich trachyandesite intrusion and flow emplaced on the southwestern margin and flank of MTS (unit Teta, 2.52±0.07 Ma, borderline trachydacite, Figs. 4, 6). The last three magmatic units have reverse magnetic polarity, whereas older Phase 3 rocks have normal polarity. Thus, the youngest magmatism of MTS captures the fundamental change in magnetic polarity at 2.58 Ma (Fig. 5; Gee and Kent, 2007).

Within the eastern Amphitheater floor, a large circular plug of fine-grained olivine gabbro (unit Qxgi, 1.98±0.05 Ma) intruded and uplifted adjacent Cretaceous rocks and caused noticeable hydrothermal alteration of both sandstone and shale (Goff et al., 2019). When viewed from the Amphitheater floor, this columnar-jointed intrusion superficially resembles the famous Devils Tower, Wyoming. It is not clear if this magma breached the surface to produce a flow. The top of the plug is somewhat vesicular (Hunt, 1938), but any flow that may have erupted from this intrusion has been completely eroded. The gabbro chemically resembles “true” basalt (≤5 wt% alkalis). This is the youngest Phase 3 magmatic event within the Amphitheater and is shown as such on Table 2 and Figure 4 even though it is a mafic intrusion.

Phase 4, terminal mafic volcanism (2.50–1.27 Ma)

Although intermediate to silicic dome and flow eruptions forming MTS ceased at 2.52 Ma, our mapping and dating campaign identified many flank eruptions of mafic flows, cones, and plugs that erupted afterward (Table 2). With few exceptions, these younger eruptions consist of trachybasalt (Fig. 4). A group of peridotite-bearing cones and flows (unit Qyxtb, 1.86–1.75 Ma) erupted from vents northwest, north and northeast of MTS (Goff et al., 2019). Three aphyric trachybasalts erupted on the north and southwest flanks of MTS (units Qyh and Qatb, 1.73, 1.77, and 1.80 Ma). These were followed by a group of distinctive fine-grained quartz-bearing trachybasalts that vented around MTS from 1.65–1.54 Ma (unit Qfqtb). The youngest mafic eruption that we could identify is the cone and flow of Cerro Pelón (unit Qyatb, 1.27±0.19 Ma).

FORMATION OF THE AMPHITHEATER

Controversy still revolves around the origin of MTS Amphitheater (Fig. 3). Four theories have been offered: 1) some form of explosion(s) (Crumpler, 2010, p. 57), 2) a lateral blast or sector collapse (Crumpler, 1982, p. 294; Crumpler, 2010), 3) glaciation (Ellis, 1935; Pierce, 2004), or 4) mass wasting/fluvial erosion (Hunt, 1938; Lipman and Mehnert, 1979; Perry et al., 1990).

First, the Amphitheater did not form from a single large explosion or series of explosions such as occurred at Valles caldera (Smith and Bailey, 1966; Goff et al., 2014b). There are no late, widespread ignimbrite (ash-flow) sheets or other pyroclastic deposits covering the 2.75 to 2.52 million-year-old landscape (i.e., the Phase 3 domes and flows) bordering the Amphitheater, and there are no late-stage circular collapse faults within the inner margins of the Amphitheater. Although non-welded pyroclastic eruptions occurred early in the development of MTS (3.10 to 2.78 Ma; Table 2; Fig. 4), they are volumetrically small (<1 km^3) and mostly restricted to paleocanyons northwest and southeast of the Amphitheater. These early pyroclastic deposits are covered by later Phase 2 dome and flow eruptions forming MTS. In contrast, our very rough estimate of the *original* volume of the Amphitheater, assuming a maximum summit elevation of 3800 m, is 9 km^3 (see below), a volume many times larger than any pyroclastic deposits we observed. This eroded material has been incorporated within the large fan of volcaniclastic sediments that flanks the east and southeast margin of the Amphitheater (see map of Goff et al., 2019).

Second, the Amphitheater did not develop from a Mount St. Helens-type lateral blast deposit (i.e., sector collapse with simultaneous magmatic explosion). Our detailed mapping of MTS identified no late-stage, blast-type pumice deposits or ignimbrites east and southeast of the volcano or elsewhere (e.g., Hoblitt et al., 1981). It is possible that relatively small sector-collapse deposits slid off some of the evolving Phase 2 domes, but we did not observe hummocky landslide or debris avalanche deposits characteristic of catastrophic stratovolcano sector collapse (Voight et al., 1981). Perhaps they are merely hidden in the more voluminous sedimentary debris flow deposits flanking the volcano. Siebert (1984) pointed out that recently formed volcanic amphitheaters formed by debris avalanches have characteristic shapes and breach width approximately equaling the crater width. In contrast, the breach width/crater width of the MTS Amphitheater is about 0.25 (Perry et al., 1990), which could be attributed to significant post-debris avalanche erosion.

Third, the Amphitheater was not carved by Pleistocene glaciation as claimed previously by Ellis (1935) and reiterated more recently by Pierce (2004). Our detailed mapping and early work by Hunt (1938) identified no glacial deposits such as moraines anywhere in or around MTS, nor did we find them above or interlayered in the upper debris flow deposits east and southeast of Water Canyon. The Amphitheater is certainly not U-shaped with a flat floor like classic glacially carved valleys (Fig. 3). More recently, Meyer et al. (2014) tried to find evidence for glaciation (including striated clasts or bedrock) but concluded that glaciation “was unlikely to have occurred for any significant period in the eastern Amphitheater of the mountain where is was previously inferred.”

Based on our recent detailed mapping in combination with new dates, we concur with Hunt (1938), Lipman and Mehnert (1979), and Perry et al. (1990) that the Amphitheater most likely developed by simple erosion of the original summit with deposition of the eroded material in the large fan of volcaniclastic sediments east of Water Canyon. Stratovolcanoes with erosional amphitheaters tend to have broad craters with narrow breaches such as observed at MTS (Siebert, 1984; Perry et al., 1990). Doming and fracturing accompanying late-stage injection of radial dikes and the trachydacite-to-alkali rhyolite plug from the composite stock in the west-central part of the volcano probably facilitated erosion. We note that the main trend of 148 radial dikes within MTS is N65°W to N25°W, or approximately parallel to the trend of the Amphitheater (Goff et al., 2019). Magma-induced hydrothermal alteration coinciding with late MTS intrusive activity was observed in many intermediate composition boulders in surrounding debris flows. This alteration likely destabilized the core of the volcano. Emplacement of the late gabbro intrusion beneath the eastern Amphitheater further damaged and weakened the edifice (Goff et al., 2019, p. 17, 29, 32-34). Erosion of the original edifice has created a large eastward-facing basin and has deposited large aprons of volcaniclastic debris around the present MTS.

HOW HIGH WAS PLIOCENE MOUNT TAYLOR

Extrapolation of the exterior morphology of MTS by Crumpler (1982, 2010) suggests the Pliocene summit was once a large bulbous dome, pyroclastic cone or combination thereof, much higher in elevation than now, perhaps as high as 4270 m (14,000 ft) or 825 m higher than today's summit. On the other hand, Perry et al. (1990) observed that present MTS has shallow exterior slope angles of 10 to 12° and contains very minor pyroclastic layers in the summit area, the latter observation verified by our mapping (Goff et al., 2019). The margin of the Amphitheater, including Mount Taylor proper and La Mosca, is composed of many coalesced domes and flows of variable elevation between 3000 and 3443 m. Extrapolation of slope angles from different points around the margin to a hypothetical maximum elevation in the past is somewhat equivocal, but it is our interpretation that MTS never exceeded 3800 m in elevation.

WHAT WAS THE VOLUME OF THE STRATOVOLCANO

Perry et al. (1990) estimated the pre-erosional volume of MTS at 23 km^3 and the volume of eroded material at 3 km^3, mostly from the Amphitheater. The geometric parameters for these calculated estimates are not given in their paper, but, in any event, these estimates seem unrealistically small to us and don't account for a maximum edifice elevation of 3800 m described above. From our recent mapping, the average diameter of MTS, including flanking mafic flows and interlayered debris flow deposits, is about ±16 km. If we assume an average base elevation of 2500 m and a maximum height of 3800 m, the relief of the volcano was once 1300 m. Inserting these values into the formula for a right circular cone, the estimated maximum volume of MTS was more reasonably about 85 km^3 with an estimated error of ±20%. The average slope angle of the original edifice was 9°, essentially equivalent to the Perry et al. (1990) calculation of 10° to 12°, but slope angles near the summit and margins of the Amphitheater are quite variable. For comparison, the estimated original volume of Mount Rainer, Washington, is about 140 km^3 (before erosion), the volume of Mount Adams, Washington, is 290 km^3, and that of Mount Shasta, California, is 350 km^3 (Orr and Orr, 1996).

WHAT WAS THE ERUPTIVE FLUX OF THE STRATOVOLCANO

From the volume of the volcano (85 km^3) and the time span of intense stratovolcano construction (0.76 Ma), we calculate an average eruptive (magmatic) flux rate of 0.11 km^3 per 10^3 years. For comparison, the eruptive flux of the San Francisco volcanic field in Arizona is 0.2 km^3 per 10^3 years (Tanaka et al., 1986), the long-lived Jemez volcanic field is 0.3 to 0.4 km^3 per 10^3 years (Gardner and Goff, 1984), and the incredibly active Mount St. Helens is 4.6 km^3 per 10^3 years (Lipman and Mullineaux, 1981). Thus, the eruptive flux of MTS is much smaller than most Cascades-type subduction zone volcanoes.

CONCLUSIONS

Major conclusions of our recent studies are:

- The summit trachyandesite lavas of MTS erupted 2.75 to 2.72 Ma and are not the youngest eruptions of the volcano. After summit activity waned, volcanism continued for another 200–230 ka around and within the edifice.
- Consequently, the youngest eruptions at MTS did not become progressively "andesitic" with time as previously thought. The summit stack of trachyandesite flows is equivalent in age to the trachydacite flow and intrusion that form La Mosca (2.71 Ma). Our dates and chemistry show that dome, flow and dike eruptions from 2.72 to 2.52 Ma are predominately trachydacite, originating from a composite stock. In fact, one of the youngest igneous events is the emplacement of the trachydacite to alkali rhyolite plug in the western Amphitheater.
- When growth of MTS ceased at 2.52 Ma, the style and chemistry of volcanism transformed to eruptions of primarily trachybasalt cones and flows surrounding the volcano. The youngest eruption anywhere near MTS is Cerro Pelón at 1.27 Ma.
- The elongate, eastward-facing Amphitheater in the approximate center of MTS formed by fluvial and mass-wasting erosional processes in Quaternary time. It did not form from large centralized explosions, from lateral blasts, or from Pleistocene glaciation of the edifice. Injection of late-stage radial dikes and various intrusive bodies and coincidental development of magma-induced hydrothermal alteration weakened the central edifice causing accelerated erosion. An alternative interpretation of precise age data could allow intrusive doming and sector collapse on the east flank to initiate erosion of the MTS amphitheater at about 2.56 Ma.
- It is our contention that the amalgam of small, coalesced flows and domes forming the original summit area of MTS never rose above 3800 m. Our estimated volume of MTS is roughly 85 km^3±20%.
- The volume and eruptive flux (0.11 km^3 per 10^3 years) of MTS was considerably smaller than presently active Cascades-type subduction zone stratovolcanoes.

ACKNOWLEDGMENTS

Geologic mapping and most research were jointly funded by STATEMAP (U.S. Geological Survey and New Mexico Bureau of Geology and Mineral Resources, (NMBGMR). High Mesa Petrographics (White Rock, New Mexico) crafted most of the thin sections. Washington State University and ALS Laboratories in Reno, Nevada, provided most of the chemical analyses. Fraser and Cathy Goff paid for some chemical analyses and thin sections and Kamilla Fellah prepared many of the samples for geochemical analysis. Richard Chamberlin and Matt Zimmerer of NMBGMR provided informative and constructive reviews of the draft manuscript. Additional reviews were obtained from Kate Zeigler (Zeigler Geologic Consulting), Virginia McLemore and Bonnie Frey (NMBGMR).

REFERENCES

Aldrich, M.J., and Laughlin, A.W., 1984, A model for the tectonic development of the southeastern Colorado Plateau boundary: Journal of Geophysical Research, v. 89, p. 10,207-10,218.

Baker, I., and Ridley, W.I., 1970, Field evidence and K, Rb, Sr data bearing on the origin of the Mount Taylor volcanic field, New Mexico, USA: Earth and Planetary Science Letters, v. 10, p. 106-114.

Cohen, K.M., Finney, S.C., Gibbard, P.L., and Fan, J.-X., 2013, The ICS international chronostratigraphic chart: Episodes, v. 36, p. 199-204.

Crumpler, L.S., 1980a, Alkali basalt through trachyte suite and volcanism, Mesa Chivato, Mount Taylor volcanic field, New Mexico: Geological Society of America Bulletin, Part I, v. 91, p. 253-255.

Crumpler, L.S., 1980b, Alkali basalt through trachyte suite and volcanism, Mesa Chivato, Mount Taylor volcanic field, New Mexico: Geological Society of America Bulletin, Part II, v. 91, p. 1293-1313.

Crumpler, L.S., 1982, Volcanism in the Mount Taylor region: New Mexico Geological Society, Guidebook 33, p. 291-298.

Crumpler, L.S., 2010, Mount Taylor, *in* Price, L.G., ed., The Geology of Northern New Mexico's Parks, Monuments, and Public Lands: Socorro, New Mexico Bureau of Geology and Mineral Resources, p. 51-60.

Dunbar, N.W., Kelley, S.A., Goff, F., and McIntosh, W.C., 2013, Rhyolitic pyroclastic deposits at Mount Taylor: Insight into early eruptive processes of a major composite volcano: New Mexico Geological Society, Guidebook 64, p. 72-74.

Dutton, C.E., 1885, Mount Taylor and the Zuni Plateau: U.S. Geological Survey, 6th Annual Report, p. 105-198.

Ellis, R.W., 1935, Glaciation in New Mexico: University of New Mexico Bulletin, Geological Series, v. 5, 31 p.

Fellah, K., 2011, Petrogenesis of the Mount Taylor volcanic field and comparison with the Jemez Mountains volcanic field, New Mexico [M.S. thesis]: Pullman, Washington State University, 92 p.

Gee, J.S., and Kent, D.V., 2007, Source of oceanic magnetic anomalies and the geomagnetic polarity timescale: London, Elsevier, Treatise on Geophysics, v. 5, p. 455-507.

Gardner, J.N., and Goff, F., 1984, Potassium-argon dates from the Jemez volcanic field: Implications for tectonic activity in the north-central Rio Grande rift: New Mexico Geological Society, Guidebook 35, p. 75-81.

Goff, F., and Kelley, S.A., 2020, Facts and hypotheses regarding the Miocene – Holocene Jemez Lineament, New Mexico, Arizona and Colorado: New Mexico Geological Society, Guidebook 71, this volume.

Goff, F., Kelley, S.A., Zeigler, K., Drakos, P., and Goff, C.J., 2008, Preliminary geologic map of the Lobo Springs 7.5-minute quadrangle map, Cibola County, New Mexico: New Mexico Bureau of Geology and Mineral Resources, Open-file Geologic Map 181, 1:24,000, http://geoinfo.nmt.edu/publications/maps/geologic/ofgm/details.cfml?Volume=181.

Goff, F., Kelley, S.A., Lawrence, J.R., and Goff, C.J., 2012, Preliminary geologic map of the Cerro Pelon 7.5 minute quadrangle, Cibola and McKinley counties, New Mexico: New Mexico Bureau of Geology and Mineral Resources, Open-file Geologic Map 202, 1:24,000, http://geoinfo.nmt.edu/publications/maps/geologic/ofgm/details.cfml?Volume=202.

Goff, F., Kelley, S.A., Lawrence, J.R., and Goff, C.J., 2014a, Preliminary geologic map of the Laguna Cañoneros 7.5 minute quadrangle, Cibola and McKinley counties, New Mexico: New Mexico Bureau of Geology and Mineral Resources, Open-file Geologic Map 244, http://geoinfo.nmt.edu/publications/maps/geologic/ofgm/details.cfml?Volume=244.

Goff, F., Warren, R.G., Goff, C.J., and Dunbar, N., 2014b, Eruption of reverse-zoned upper Tshirege Member, Bandelier Tuff from centralized vents within Valles caldera, New Mexico: Journal of Volcanology and Geothermal Research, v. 276, p. 82-104.

Goff, F., Kelley, S.A., Goff, C.J., McCraw, D.J., Osburn, G.R., Lawrence, J.R., Drakos, P.G., and Skotnicki, S.J., 2019, Geologic map of the Mount Taylor volcano area, New Mexico: New Mexico Bureau of Geology and Mineral Resources, Geologic Map 80, 1:36,000 scale (color) w/ 57 page booklet.

Hallett, R.B., Kyle, P.R. and McIntosh, W.C., 1997, Paleomagnetic and $^{40}Ar/^{39}Ar$ age constraints on the chronologic evolution of the Rio Puerco volcanic necks and Mesa Prieta, west-central New Mexico: Implications for transition zone magmatism: Geological Society of America Bulletin, v. 109, p. 95-106.

Hoblitt, R.P., Miller, D.C., and Vallance, J.W., 1981, Origin and stratigraphy of the deposit produced by the May 18 directed blast, *in* Lipman, P.W., and Mullineaux, D.R., eds., The 1980 eruptions of Mount St. Helens, Washington: U.S. Geological Survey, Professional Paper 1250, p. 401-419.

Hoffman, G.K., 2017, Coal Resources, *in* McLemore, V.T., Timmons, S., and Wilks, M., eds., Energy and Mineral Resources of New Mexico: New Mexico Bureau of Geology and Mineral Resources, Memoir 50B, 65 p.

Hunt, C.B., 1938, Igneous geology and structure of the Mount Taylor volcanic field, New Mexico: U.S. Geological Survey, Professional Paper 189-B, p. 51-80.

Irvine, T.N., and Baragar, W.R.A., 1971, A guide to the chemical classification of the common volcanic rocks: Canadian Journal of Earth Science, v. 8, p. 523-548.

Kelley, V.C., 1963, Geology and technology of the Grants uranium region: New Mexico Bureau of Mines and Mineral Resources, Memoir 15, 277 p.

Kelley, S., Dunbar, N., McIntosh, W., and Goff, F., 2013, Third day road log: trip 2 – tuffs of San Mateo Canyon: New Mexico Geological Society, Guidebook 64, p. 70-72.

Kuiper, K.F., Deino, A., Hilgen, H.J., Krijgsman, W., Renne, P.R., and Wijbrans, J.R., 2008, Synchronizing rock clocks of earth history: Science, v. 320, p. 500-504.

Le Bas, M.J., Le Maitre, R.W., Streckeisen, A., and Zanettin, B., 1986, A chemical classification of volcanic rocks based on the total alkali-silica diagram: Journal of Petrology, v. 27, p. 745-750.

Lipman, P.W., and Mehnert, H.H., 1979, Potassium-argon ages from the Mount Taylor volcanic field, New Mexico: U.S. Geological Survey, Professional Paper 1124-B, 8 p.

Lipman, P.W., and Moench, R.H., 1972, Basalts of the Mt. Taylor volcanic field, New Mexico: Geological Society of America Bulletin, v. 83, p. 1335-1344.

Lipman, P.W., and Mullineaux, D.R., 1981, The 1980 eruptions of Mount St. Helens, Washington: U.S. Geological Survey, Professional Paper 1250, 844 p.

Luedke, R.G., and Smith, R.L., 1978, Map showing distribution, composition, and age of late Cenozoic volcanic centers in Arizona and New Mexico: U.S. Geological Survey, Miscellaneous Investigations Series Map I-1091-A.

Mayo, E.B., 1958, Lineament tectonics and some ore districts of the southwest: Transactions American Institute of Metallurgical Engineers, v. 211, p. 1169-1175.

McCraw, D.J., Read, A.S., Lawrence, J.R., Goff, F., and Goff, C.J., 2009, Preliminary geologic Map of the San Mateo 7.5 minute quadrangle, McKinley and Cibola counties, New Mexico: New Mexico Bureau of Geology and Mineral Resources Open-file Geologic Map 194, http://geoinfo.nmt.edu/publications/maps/geologic/ofgm/details.cfml?Volume=194.

McLemore, V.T., 2011, The Grants uranium district: Update on source, deposition, and exploration: The Mountain Geologist, v. 48, p. 23-44.

McLemore, V.T., and Chenoweth, W.L., 2017, Uranium Resources, *in* McLemore, V.T., Timmons, S., and Wilks, M., eds., Energy and Mineral Resources of New Mexico: New Mexico Bureau of Geology and Mineral Resources, Memoir 50C, 67 p.

Meyer, G.A., Muir Watt, P., and Wilder, M., 2014, Was Mount Taylor glaciated in the late Pleistocene? An analysis based on field evidence and regional equilibrium line altitudes: New Mexico Geology, v. 36, p. 32-39.

Olsen, K.H., Keller, G.H., and Stewart, J.N., 1979, Crustal structure along the Rio Grande rift from seismic refraction profiles, *in* Riecker, R.E., ed., Rio Grande Rift: Tectonics and Magmatism: Washington, D.C., American Geophysical Union, p. 127-143.

Olsen, K.H., Baldridge, W.S., and Callender, J.F., 1987, Rio Grande rift: An overview: Tectonophysics, v. 143, p. 119-139.

Orr, E.L., and Orr, W.N., 1996, Geology of the Pacific Northwest: New York, McGraw Hill, 115 p.

Osburn, G.R., Kelley, S.A., and Goff, F., 2010. Preliminary geologic map of the Mount Taylor 7.5- minute quadrangle, Cibola County, New Mexico: New Mexico Bureau of Geology and Mineral Resources Open-file Geologic Map 186, scale 1:24,000, http://geoinfo.nmt.edu/publications/maps/geologic/ofgm/details.cfml?Volume=186.

Owen, D.E., and Owen, D.E., Jr., 2003, Stratigraphy of the Dakota Sandstone and intertongued Mancos Shale along the southern flank of the San Juan

Basin, west-central New Mexico: New Mexico Geological Society, Guidebook 54, p. 325-330.

Perry, F. V., Baldridge, W. S., DePaolo, D. J., and Shafiqullah, M., 1990, Evolution of a magmatic system during continental extension: The Mount Taylor volcanic field, New Mexico: Journal of Geophysical Research, v. 95, p. 19,327-19,348.

Pierce, K.L., 2004, Pleistocene glaciations of the Rocky Mountains, *in* Gillespie, A.R., Porter, S.C., and Atwater, B.F., eds., The Quaternary Period in the United States: Amsterdam, Elsevier, Developments in Quaternary Science 1, p. 63-76.

Sears, J.D., Hunt, C.B., and Hendricks, T.A., 1941, Transgressive and regressive Cretaceous deposits in southern San Juan Basin, New Mexico. U.S. Geological Survey, Professional Paper 193-F, p., 101-121.

Siebert, L., 1984, Large volcanic debris avalanches: Characteristics of source areas, deposits and associated eruptions: Journal of Volcanology and Geothermal Research, v. 22, p. 163-197.

Skotnicki, S.J., Drakos, P.G., Goff, F., Goff, C.J., and Riesterer, J., 2012, Preliminary geologic map of the Seboyeta 7.5-minute quadrangle, Cibola County, New Mexico: New Mexico Bureau of Geology and Mineral Resources, Open-file Geologic Map 226, scale 1:24,000, http://geoinfo.nmt.edu/publications/maps/geologic/ofgm/details.cfml?Volume=226.

Smith, R.L., and Bailey, R.A., 1966, The Bandelier Tuff: A study of ash-flow eruption cycles from zoned magma chambers: Bulletin of Volcanology, v. 29, p. 83-104.

Sosa, A., Thompson, L., Velasco, A.A., Romero, R., and Herrmann, R., 2014, 3-D structure of the Rio Grande rift from 1-D constrained joint inversion of receiver functions and surface wave dispersion: Earth and Planetary Science Letters, v. 402, p. 127-137.

Tanaka, K.L, Shoemaker, E.M., Ulrich, G.E., and Wolfe, E.W., 1986, Migration of volcanism in the San Francisco volcanic field: Geological Society of America Bulletin, v. 97, p. 129-141.

Thompson, G.A., and Zoback, M.L., 1979, Regional geophysics of the Colorado Plateau: Tectonophysics, v. 61, p. 149-181.

Voight, B., Glicken, H, Janda, R.J., and Douglass, P.M., 1981, Catastrophic rock slide avalanche of May 18, *in* Lipman, P.W., and Mullineaux, D.R., eds., The 1980 eruptions of Mount St. Helens, Washington: U.S. Geological Survey, Professional Paper 1250, p. 347-377.

Wilson, M., 1989, Igneous Petrogenesis: London, Unwin Hyman, 466 p.